Scientia Iranica A (2023) 30(3), 860–876

SCIENTIA IRANICA

Sharif University of Technology
Scientia Iranica
Transactions A: Civil Engineering
http://scientiairanica.sharif.edu

Parametric investigations into dynamics of cracked thin rectangular plates excited by a moving mass

A. Nikkhoo[a,*], Sh. Banihashemi[a], and K. Kiani[b]

a. *Departement of Civil Engineering, University of Science and Culture (USC), Tehran, P.O. Box 13145-871, Iran.*
b. *Departement of Civil Engineering, K.N. Toosi University of Technology, Tehran, Iran.*

Received 17 May 2021; received in revised form 20 April 2022; accepted 27 June 2022

KEYWORDS
Cracked thin plate;
Dynamic vibration;
Moving load;
Moving mass;
Orthogonal polynomials;
Eigenfunction expansion method.

Abstract. Dynamic analysis of cracked thin rectangular plates subjected to a moving mass is investigated first in this paper. To this end, the eigenfunction expansion method is employed to solve the ruling differential equation of motion. For the first time, intact plate orthogonal polynomials in combination with well-known corner functions, serving as a composition, have been used in the governing equation which required professional computer programming to solve the equation. The proposed solutions afford upper bounds for true solutions, which is a property of an appropriate numerical solution. Parametric investigations are performed to determine the effects of moving mass weights, moving mass velocities, crack lengths, crack angular orientations, and plates' aspect ratios on the dynamic responses of cracked thin rectangular plates. The results confirm that the moving mass has a greater impact than the moving load on the dynamic responses of cracked thin rectangular plates. Furthermore, there are non-monotonous nonlinear relations between altering dynamic responses of cracked thin rectangular plates with various boundary conditions and modifying moving mass weights, moving mass velocities, crack lengths, inclined crack angles, and plates' aspect ratios.

1. Introduction

Rectangular plates including large-span bridges and concrete floor slabs are commonly used in civil structures. Irregular dynamic loads, especially cyclic loads, initiate cracks in plates, affecting the performance of structures. Therefore, it is of utmost importance to study cracked plates subjected to various dynamic excitations.

Free vibrations of rectangular plates with simply supported boundary conditions including a crack parallel to one of the edges were studied by many researchers. Few papers in the literature have analyzed cracked rectangular plates under various boundary conditions. Many researchers have investigated cracked rectangular plates including simply supported as well as clamped boundary conditions. Utilizing Levy's model of the solution, Lynn and Kumbasar [1] proposed a solution using Green's functions, while Stahl and Keer [2] represented dual series equations, reduced to homogeneous Fredholm integral equations of second type. Solecki [3] provided a solution by means of the finite Fourier transformation of discontinuous functions, derived from the Navier's model of the solution. Obtaining free vibration solutions of cracked plates with complex geometries and boundary conditions, researchers employed numerical methods such as Finite Element Methods (FEMs) or the Ritz method. Qian et al. [4] and Krawczuk [5] presented finite element solutions. Qian et al. [4] integrated the stress intensity factor of cracked plates subjected to

*. *Corresponding author. Tel.: +98 21 44252045*
E-mail address: nikkhoo@usc.ac.ir (A. Nikkhoo)

doi: 10.24200/sci.2022.58345.5686

twisting, bending, and shearing to obtain the stiffness matrix of an element with a crack, while Krawczuk's approach was expressed in a closed form.

Bachene et al. [6] developed an extended finite element solution based on the first-order shear deformation plate theory. By utilizing FEMs to analyze the vibrations of cracked thin plates, the basis of the classical plate theory and constructing C^1-type elements can overcome difficulties; or, by using FEMs to obtain vibrations of cracked thin plates basis of the first-order shear deformation plate theory and forming C^0 type elements, one can resolve the problem of shear locking. Since the well-known Ritz method was presented, it has often used. Through the instrumentality of the Ritz method and domain decomposition approach, Yuan and Dickinson [7], Liew et al. [8], and Lee and Lim [9] obtained the results of natural frequencies and mode shapes of thin central cracked rectangular plates with simply supported boundary conditions. Utilizing the Ritz method, Huang et al. [10–12] proposed natural frequencies of simply supported rectangular thin plates with side cracks [10] and internal cracks [11], as well as those simply supported rectangular thick plates or Mindlin plates with side cracks or internal cracks [12] at arbitrary locations with different crack lengths and various crack angular orientations. Riks et al. [13], Barut et al. [14], and Brighenti [15,16] investigated the buckling behavior of cracked rectangular plates via FEMs. Zeng et al. [17] proposed solutions of vibrations and stabilities of side cracked rectangular plates, and Xue et al. presented solutions of vibrations and stabilities of flat stiffened side-cracked plates [18], as well as preloaded cracked rectangular Mindlin plates [19]. Huang et al. investigated the buckling of internally cracked square plates [20], while Xue et al. analyzed the vibrations and buckling responses of cracked rectangular Mindlin plates [21]. Huang et al. studied the vibrations and buckling responses of three-dimensional (3D) internal and side-cracked Functionally Graded Material (FGM) plates [22] as well as preloaded 3D internal and side-cracked FGM plates [23] by means of the Ritz method and admissible corner functions formed by the moving least-squares approach or the MLS-Ritz method. Kiani and Żur [24] investigated vibrations of double parallel defected nanorods by utilizing the nonlocal surface energy principium and the Galerkin method.

According to the existing studies in the literature, free vibrations of the cracked plates, or vibrations of cracked plates subjected to static loads, were investigated. However, the researchers [25–36] reported that dynamic excitations such as moving loads and particularly moving masses, whose inertial effects were taken into account, had impacts on plate displacement. The investigation of plates subjected to a moving load was initiated in the 1970s. Mote [25] first studied the vibration of the centrally clamped annulus plate with the encircled free boundary conditions subjected to two orbiting moving loads: (a) a harmonic load at an unalterable angular velocity and (b) a load whose speed was the sum of a harmonic and an unalterable component. Abundant studies on beams and rectangular plates subjected to a moving load were collected in a book by Fryba [26]. Cifuentes and Lalapet [27] investigated the dynamic response of an arbitrary plate subjected to an orbiting mass. They utilized the technique basis of the finite element discretization of the plate, whose mesh consisted of the circumnavigating mass trajectory. The results highlighted the consequence of the inertia of the moving mass. Shadnam et al. [28] explored simply supported Kirchhoff rectangular plates subjected to a moving mass. The eigenfunction expansion method was applied to solve the differential equation of motion. In the mentioned investigation, only the vertical acceleration component of the moving mass was considered. The results showed that the moving mass inertia and the participation of each vibration mode affected the dynamic responses of plates, particularly in case of larger velocities and/or larger mass weights. Rofooei and Nikkhoo [29] obtained the responses of thin rectangular plates subjected to a moving mass by utilizing all acceleration elements of the moving mass. The dynamic responses were reduced via piezoelectric patches as controllers. The results indicated the efficacy of the moving mass inertia. In another study, the dynamic responses of thin rectangular plates with varied boundary conditions subjected to a moving mass were investigated by Nikkhoo and Rofooei [30]. They revealed the importance of the inertial effect by utilizing all acceleration parts of the moving mass compared to applying only the vertical acceleration component of the moving mass. Kiani [31–33] scrutinized the embedded nanoplate vibration modeled based on the nonlocal continuum theory of Eringen, subjected to biaxial loads. Moving nanoparticles were modeled as rigid bodies, whose frictions were taken into account. The results proved the inertial effect, the effect of the length to the thickness ratio of the nanoplate, the velocities or angular velocities of moving nanoparticles, as well as the effect of the lateral stiffness of the surrounded medium on the displacement time history of a nanoplate. According to the effect of multi-moving masses across plates, Nikkhoo et al. [34] employed the eigenfunction expansion method to evaluate the resonance of a thin rectangular plate subjected to a series of moving masses. The results indicated the import of load inertias and load velocities. Rofooei et al. [35] compared the Von Karman with the Kirchhoff plate theory to investigate the displacement of rectangular plates subjected to a moving mass. They reported that smaller deflections were obtained by applying the Von Karman plate theory than the Kirchhoff plate theory. Nikkhoo et al. [36] proposed accurate results of vibrations of flexo-poroelastic structures on elastic beds subjected to moving loads.

The present study first obtained dynamic responses of thin rectangular plates with internal cracks at arbitrary locations featuring different crack lengths and inclined crack angles with various boundary conditions subjected to a moving mass. Accordingly, the eigenfunction expansion method is utilized to transform the partial differential equation of motion into a number of connected normal differential equations. For the first time, intact plate orthogonal polynomials combined with admissible corner functions are applied in the eigenfunction expansion method formulations. The admissible corner functions are able to define stress singularities near the tips of the crack and to describe the discontinuities due to the crack line. Professional computer programming is employed to solve the governing equations. Furthermore, parametric studies are conducted to specify effects of moving mass weighs, moving mass velocities, crack lengths, inclined crack angles, and plates' aspect ratios on dynamic responses of cracked plates. Consequently, there are non-monotonous nonlinear relationships between varying dynamic responses of cracked thin rectangular plates with various boundary conditions and altering the mentioned parameters respectively.

2. Problem formulations

The present study utilized the formulas composed of the reference equations. While these formulations are similar to a composition, they are presented in the form of a collection.

The partial differential equation of motion of an undamped uniform thin rectangular plate subjected to a moving mass is expressed as follows:

$$D\nabla^4 W(x,y,t)+m\frac{\partial^2 W(x,y,t)}{\partial t^2} = M\left(-g-\frac{d^2W(x_0(t),y_0(t),t)}{dt^2}\right) \delta(x-x_0(t))\delta(y-y_0(t)), \quad (1)$$

where $d^2W(x_0(t),y_0(t),t)/dt^2$ is the moving mass acceleration obtained from the total differentiation of the second order of $W(x_0(t),y_0(t),t)$, which is the contact curve between the plate and the moving mass at any time t at the time-dependent coordinates x_0 and y_0. $W(x,y,t)$ is the vertical deflection of the plate at any time-dependent coordinates x,y.

$D=\frac{Eh^3}{12(1-\nu^2)}$ is the plate's flexural rigidity, where E, ν, and h are the plate's modulus of elasticity, Poisson's ratio, and thickness, respectively. Accordingly, g, m, M, and δ are the gravity's acceleration, the mass per unit area of the plate, the moving load's magnitude, and the Dirac-delta function, respectively. The eigenfunction expansion method is utilized to solve the equation of motion. The free vibration response of the plate is assumed as:

$$W(x,y,t)=\sum_{l=1}^{\infty}\phi_l(x,y)e^{\bar{i}\omega_l t}, \quad (2)$$

in which $\phi_l(x,y), \omega_l$, and $\bar{i}$ are the lth mode shape, the natural frequency of the plate, and the imaginary unit, respectively. It is assumed that the mode shape of the plate, $\phi_l(x,y)$, is considered. While the mode shape of the plate must consider the plate's boundary condition form and satisfy the differential equation, according to the Ritz method, the mode shape is represented as two sets of the functions summation:

$$\phi_l(x,y)=\phi_p(x,y)+\phi_c(x,y), \quad (3)$$

where $\phi_p(x,y)$ denotes the behavior of the intact plate in which:

$$\phi_p(x,y)=\sum_{i=1}^{N}a_i\phi_i(x,y), \quad (4)$$

where $\phi_i(x,y)$ is a set of orthogonal polynomials in x and y directions (Figure 1) generated by the Gram-Schmidt process [37] expressed according to the Boundary Characteristics Orthogonal Polynomials (BCOP) method [38]. N is the number of utilized orthogonal polynomials and a_i is a set of constants denoting the participation contribution ratio of the orthogonal polynomials.

Figure 1 reveals a thin rectangular plate with a crack subjected to a moving mass with the magnitude M. The indicated polar coordinates (r_1, θ_1) and (r_2, θ_2) are the two tips of an internal crack. a_0 and b_0 are the crack center coordinates in x and y directions, respectively. a, b, c, and θ are the rectangular cracked plate length, the rectangular cracked plate width, the crack length, and the inclined crack angle, respectively.

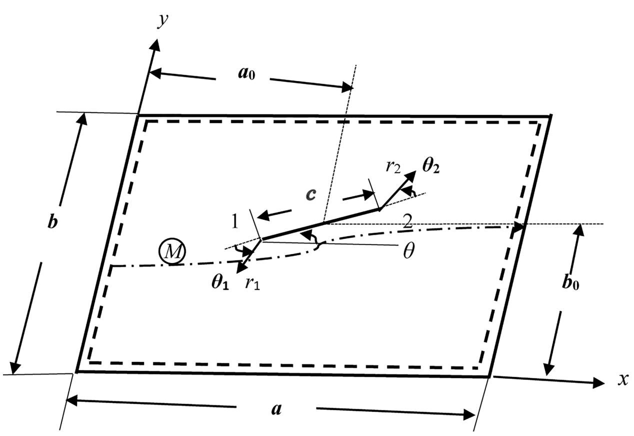

Figure 1. A rectangular plate with a crack subjected to a moving mass (a_0 and b_0 are determined as a crack center coordinates).

$\phi_c(x,y)$ are the William's solutions for the plate's internal crack, denoting the well-known corner functions, explaining the behavior of the cracked plate along the crack line as additive modes, describing the stress singularity near the tips of the crack and the discontinuities along the crack:

$$\phi_c(x,y) = x^{n_1}(1-x)^{n_2}y^{n_3}(1-y)^{n_4} \left\{ \sum_{n=1}^{N_1} b_n\phi_{n,S}(\gamma_n,r_1,\theta_1,r_2,\theta_2) + \sum_{n=1}^{N_2} c_n\phi_{n,A}(\gamma_n,r_1,\theta_1,r_2,\theta_2) + \sum_{n=1}^{N_3} c_n\phi_{n,A}(\gamma_n,r_1,\theta_1,r_2,\theta_2) + \sum_{n=1}^{N_4} e_n\phi_{n,S}(\gamma_n,r_2,\theta_2,r_1,\theta_1) \right\}, \tag{5}$$

in which:

$$\gamma_n = n/2, \qquad n=1,2,\cdots, \tag{6-a}$$

and for ($\gamma_n \in \mathbb{N}$ natural numbers):

$$\phi_{n,S}(\gamma_n,r_1,\theta_1,r_2,\theta_2) = r_j^{\bar{k}} r_i^{\gamma_n+1} \left(-\frac{\lambda_2}{\lambda_1}\cos(\gamma_n+1)\theta_i + \cos(\gamma_n-1)\theta_i\right), \tag{6-b}$$

$$\phi_{n,A}(\gamma_n,r_1,\theta_1,r_2,\theta_2) = r_j^{\bar{k}} r_i^{\gamma_n+1} \left(\frac{\lambda_3}{\lambda_1}\sin(\gamma_n+1)\theta_i + \sin(\gamma_n-1)\theta_i\right), \tag{6-c}$$

and for $\gamma_n \notin \mathbb{N}$ (natural numbers):

$$\phi_{n,S}(\gamma_n,r_1,\theta_1,r_2,\theta_2) = \sin^2(\theta_j/2) r_j^{k} r_i^{\gamma_n+1} \left(\frac{\lambda_3}{\lambda_1}\cos(\gamma_n+1)\theta_i + \cos(\gamma_n-1)\theta_i\right), \tag{6-d}$$

$$\phi_{n,A}(\gamma_n,r_1,\theta_1,r_2,\theta_2) = \sin^2(\theta_j/2) r_j^{k} r_i^{\gamma_n+1} \left(-\frac{\lambda_2}{\lambda_1}\sin(\gamma_n+1)\theta_i + \sin(\gamma_n-1)\theta_i\right), \tag{6-e}$$

where:

$$\lambda_1 = (\gamma_n+1)(\nu+1),$$

$$\lambda_2 = -\gamma_n(1-\nu) + (3+\nu),$$

$$\lambda_3 = \gamma_n(1-\nu) + (3+\nu). \tag{6-f}$$

The subscripts A and S denote antisymmetric and symmetric modes, respectively. n_1, n_2, n_3, and n_4 determine the boundary conditions of the cracked plate that are satisfied as 2, 1, or 0, denoting the three geometrical boundary conditions as clamped, simply supported, and free, respectively. N_1, N_2, N_3, and N_4 are the number of employed admissible corner functions. b_n, c_n, d_n, and e_n are the constants that denote the participation contribution ratio of the admissible corner functions. From Eq. (2), one can deduce the following:

$$D\nabla^4\phi_l(x,y) = \mu\omega_l^2\phi_l(x,y). \tag{7}$$

An arbitrary forced response of the cracked plate is defined as follows:

$$W(x,y,t) = \sum_{l=1}^{N} \phi_l(x,y)S_l(t), \tag{8}$$

where $S_l(t)$ is the time-dependent modal amplitude of the cracked plate. Eqs. (2), (3), and (7) are substituted into the equation of motion. By normalizing and re-arranging the obtained equation in the matrix form, the following is obtained:

$$\mathbf{M}(t)\ddot{s}(t) + \mathbf{C}(t)\dot{s}(t) + \mathbf{K}s(t) = \mathbf{F}(t)$$

$$s(t_0) = s_0, \qquad \dot{s}(t_0) = s_{10}, \tag{9}$$

$$M_{ij} = \delta_{ij} + Mw_i(x_0(t),y_0(t)) [w_j(x_0(t),y_0(t))], \tag{10-a}$$

$$C_{ij} = 2Mw_i(x_0(t),y_0(t))[\dot{x}_0(t)w_{j,x}(x_0(t),y_0(t)) + \dot{y}_0(t)w_{j,y}(x_0(t),y_0(t))], \tag{10-b}$$

$$K_{ij} = \omega^2\delta_{ij} + Mw_i(x_0(t),y_0(t)) [\dot{x}_0^2 w_{j,xx}(x_0(t),y_0(t)) + \dot{y}_0^2 w_{j,yy}(x_0(t),y_0(t)) + \ddot{x}_0(t)w_{j,x}(x_0(t),y_0(t)) + \ddot{y}_0(t)w_{j,y}(x_0(t),y_0(t)) + 2\dot{x}_0(t)\dot{y}_0(t)w_{j,xy}(x_0(t),y_0(t))], \tag{10-c}$$

$$F_j = -Mgw_j(x_0(t),y_0(t)), \tag{10-d}$$

$$s(t) = \begin{bmatrix} s_1(t) \\ s_2(t) \\ . \\ . \\ . \\ s_N(t) \end{bmatrix}_{N\times 1}, \tag{10-e}$$

where s_0 and s_{10} are the initial conditions. Utilizing the state-space form of Eq. (9) yields:

$$\dot{\mathbf{A}}(t) = \mathbf{G}(t)\mathbf{A}(t) + \bar{\mathbf{F}}(t), \tag{11}$$

where:

$$\mathbf{A}(t)=\begin{bmatrix} s(t)\\ \dot{s}(t)\end{bmatrix}_{2N\times 1},$$

$$\mathbf{G}(t)=\begin{bmatrix} \mathbf{0} & \mathbf{I}\\ -\mathbf{M}^{-1}\mathbf{K} & -\mathbf{M}^{-1}\mathbf{C}\end{bmatrix}_{2N\times 2N},$$

$$\bar{\mathbf{F}}(t)=\begin{bmatrix} \mathbf{0}\\ \mathbf{M}^{-1}\mathbf{F}\end{bmatrix}_{2N\times 1}. \tag{12}$$

Eq. (11) is solved as follows:

$$\mathbf{A}(t)=\mathbf{V}(t)\mathbf{V}^{-1}(t_0)\mathbf{A}(t_0)+\int_{t_0}^{t}\{\mathbf{V}(t)\mathbf{V}^{-1}(\tau)[\bar{\mathbf{F}}(\tau)]\}d\tau, \tag{13}$$

where $\mathbf{V}(t)$ is the fundamental solution matrix:

$$\dot{\mathbf{V}}(t)=\mathbf{G}(t)\mathbf{V}(t),\quad \mathbf{V}(t_0)=\mathbf{I}_{2k},$$

$$\mathbf{A}(t)=\mathbf{V}(t)\mathbf{A}(t_0). \tag{14}$$

A transfer matrix $\bar{\mathbf{V}}(t)$ is employed to obtain $\mathbf{V}(t)$:

$$\bar{\mathbf{T}}(t,\tau)\approx\mathbf{V}(t)\mathbf{V}^{-1}(\tau). \tag{15}$$

Therefore, we have:

$$\mathbf{A}(t)=\bar{\mathbf{T}}(t,\tau)\mathbf{A}(\tau). \tag{16}$$

An approximate solution is utilized to obtain $\bar{\mathbf{T}}$:

$$\bar{\mathbf{T}}(t_{q+1},t_q)=e^{\mathbf{G}(t_q)\Delta t_q}, \tag{17}$$

Δt_q is defined as the time interval and $\mathbf{G}$ is nonsingular. Therefore, a solution to Eq. (11) obtains:

$$\mathbf{A}_1(t_{q+1})=\mathbf{G}_1(t_q)\mathbf{A}(t_q)+\bar{\mathbf{F}}_1(t_q), \tag{18}$$

where:

$$\mathbf{G}_1(t_q)\cong e^{\mathbf{G}(t_q)\Delta t_q}, \tag{19}$$

$$\bar{\mathbf{F}}_1(t_q)\cong[\mathbf{G}_1(t_q)-\mathbf{I}]\mathbf{G}^{-1}(t_q)\bar{\mathbf{F}}(t_q). \tag{20}$$

The present method can be extended to solve complexed and composited dynamic loadings by utilizing the Betti and Lord Rayleigh reciprocity theorem and the superposition method. It can also solve the presented problem for cracked plates with other shapes by altering the coordinates. The mentioned method can be utilized to solve the mentioned problem for plates with multiple cracks, by setting admissible functions to each crack. It can be also extended to such problems for Mindlin cracked plates, by setting new admissible functions in the 3D formulation. The presented method can solve the mentioned problem for cracked plates rested on the Winkler foundation, by adding $KW(x,y,t)$ to the left side of Eq. (1) and adding $K\delta_{ij}$ to the right side of Eq. (10-c), where K is the modulus of the Winkler foundation.

3. The verification and the numerical examples of the present investigation

Since the issue of cracked plates subjected to a moving mass has not been investigated in the publicized literature, the efficiency of the presented method is determined by verifying the obtained results of the natural frequencies of a simply supported cracked square plate and the spectra of a simply supported square intact plate subjected to a moving mass. To this end, the approach proposed in Section 2 is utilized to solve the problem. After the convergence investigation, spectra of cracked plates with various boundary conditions subjected to a moving mass are presented and parametric studies are performed. As an extension of the suggested approach, spectra of elastically rested cracked plates subjected to a moving mass are investigated and parametric studies are proposed. The Winkler foundation as an elastic foundation is reacted at the bottom of cracked plates. The average modulus of Winkler foundation is designated $K=10^6$ N/m^3 [40,41] depending on the properties of the subgrade. The MATLAB program is utilized to conduct numerical analyses. For the convergence study of the frequencies, the first 25 vibration modes of an intact plate in combination with 60-term admissible corner functions ($n=15$) are considered. Table 1 presents the convergence investigation of the frequency parameters $\lambda=\omega a^2\sqrt{\rho h/D}$ for a simply supported square plate with the horizontal center crack ($c/a=0.8$, $a_0/a=b_0/b=0.5$, $\theta=0°$).

Table 2 presents the convergence investigation of the frequency parameters λ for a simply supported square plate with the horizontal and inclined center cracks ($c/a=0.5$, $a_0/a=b_0/b=0.5$, $\theta=0°$, and $\theta=45°$).

Table 1. The frequency parameters for a simply supported square cracked plate ($c/a=0.8$, $a_0/a=b_0/b=0.5$, $\theta=0°$).

Mode number	Present study	Huang et al. [11]	Stahl and Keer [2]	Liew et al. [8]
1	16.4316	16.41	16.4	16.47
2	27.7489	27.77	27.77	27.43
3	47.2229	47.21	47.26	47.27

Table 2. The frequency parameters for a simply supported square cracked plate ($c/a = 0.5$, $a_0/a = b_0/b = 0.5$, $\theta = 0°$as well as $\theta = 45°$).

Mode number	Present study $\theta = 0°$	Huang et al. [11] $\theta = 0°$	Present study $\theta = 45°$	Huang et al. [11] $\theta = 45°$
1	17.60	17.72	17.03	17.53
2	43.93	43.06	43.49	42.85
3	49.01	48.69	49.00	48.33

The results of Tables 1 and 2 reveal that the present results ensure that the upper bounds are the true solutions and this is one grave aspect of a worthy numerical solution.

For the convergence investigation of the moving mass effect, the aluminum thin square plate with the simply supported boundary conditions featuring the modulus of elasticity $E = 7.31 \times 10^{10}$ Pa, the mass density $\rho = 2700$ kgm^{-3}, and Poisson's ratio $\nu = 0.33$ is taken into account. Accordingly, the width and the length of the plate are equal to 2 m and its thickness is 1.7 cm. The first 25 vibration modes are taken into consideration. It is assumed that a moving mass with different velocities and mass weights takes a rectilinear direction. In other words, $x_0(t) = vt$ and $y_0(t) = b/2$, where v denotes the velocity of the moving mass.

Figure 2 indicates the accuracy of the inertial effect on Dynamic Amplification Factors (DAFs) of the simply supported square plate due to alterations of mass weights and mass velocities. Depending on mass velocities, maximum dynamic responses may occur at the first phase of passing, while the mass is still on the plate or at the second phase. The mass already passed, indicating a free vibration. $v' = 2a/T_1$ is the velocity parameter. Herein, T_1 is the vibration period of the first plate. According to the loading safety factor, the moving mass weight whose inertial effect is considered is designated to enhance the mass weight of the structure to 0.45. In order to ensure the stability of the dynamic system, the mass velocities correspond to the characteristic equation or the frequency equation [42], the positive root for natural frequencies, the positive definition of the structure's mass as well as the structure's stiffness, and the formula for natural frequencies of a simply-supported plate [30,43],

$$\omega_n = \omega_{ij} = \pi^2 \left[\left(\frac{i}{a}\right)^2 + \left(\frac{j}{b}\right)^2 \right] \sqrt{\frac{D}{m}} = \frac{2\pi}{T_n}$$

is limited to:

$$\frac{\pi\left(1+\alpha^2\right)}{2\sqrt{\alpha}}\sqrt{\frac{D}{M}}.$$

After verifying the accuracy and the convergence of this method, studies of moving mass effects and parametric analysis of cracked plates and elastically rested cracked plates are carried out. An aluminum thin cracked plate with various boundary conditions featuring the modulus of elasticity $E = 7.31 \times 10^{10}$ Pa, the mass density $\rho = 2700$ kgm^{-3}, and Poisson's ratio $\nu = 0.33$ is considered. The width is 2 m, the length varies, and the thickness is 1.7 cm such that the aspect ratio of the plate, $\alpha = a/b$, is at 1/2 to 2. The first 25 vibration modes of intact plates in combination with 20-term admissible corner functions ($n = 5$) are considered.

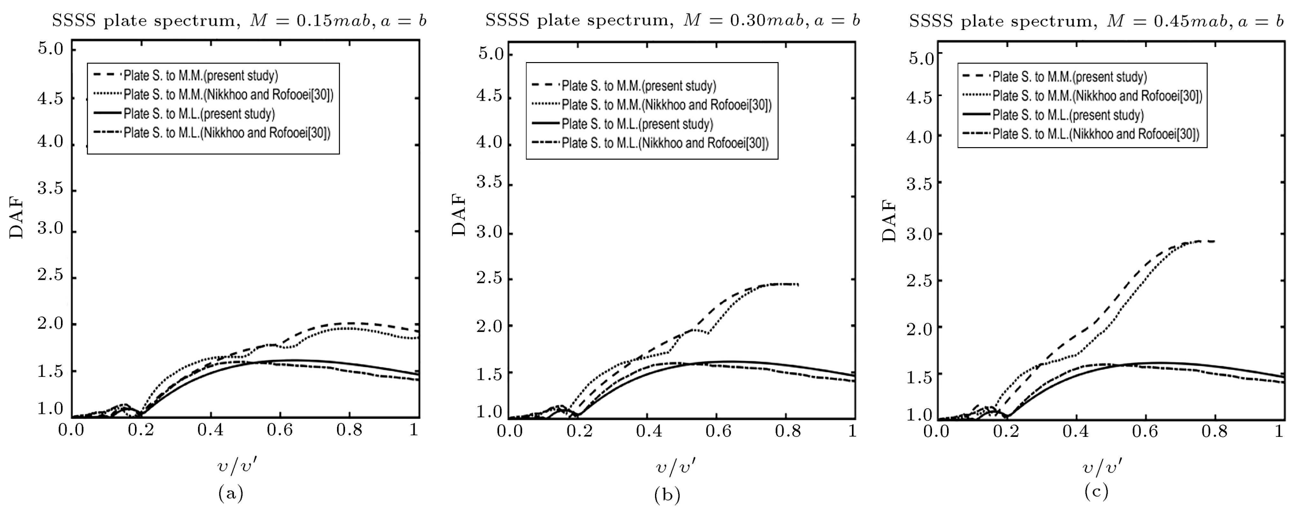

Figure 2. The effect of the inertia on the DAFs of the SSSS square plate due to the velocity and the mass weight variations.

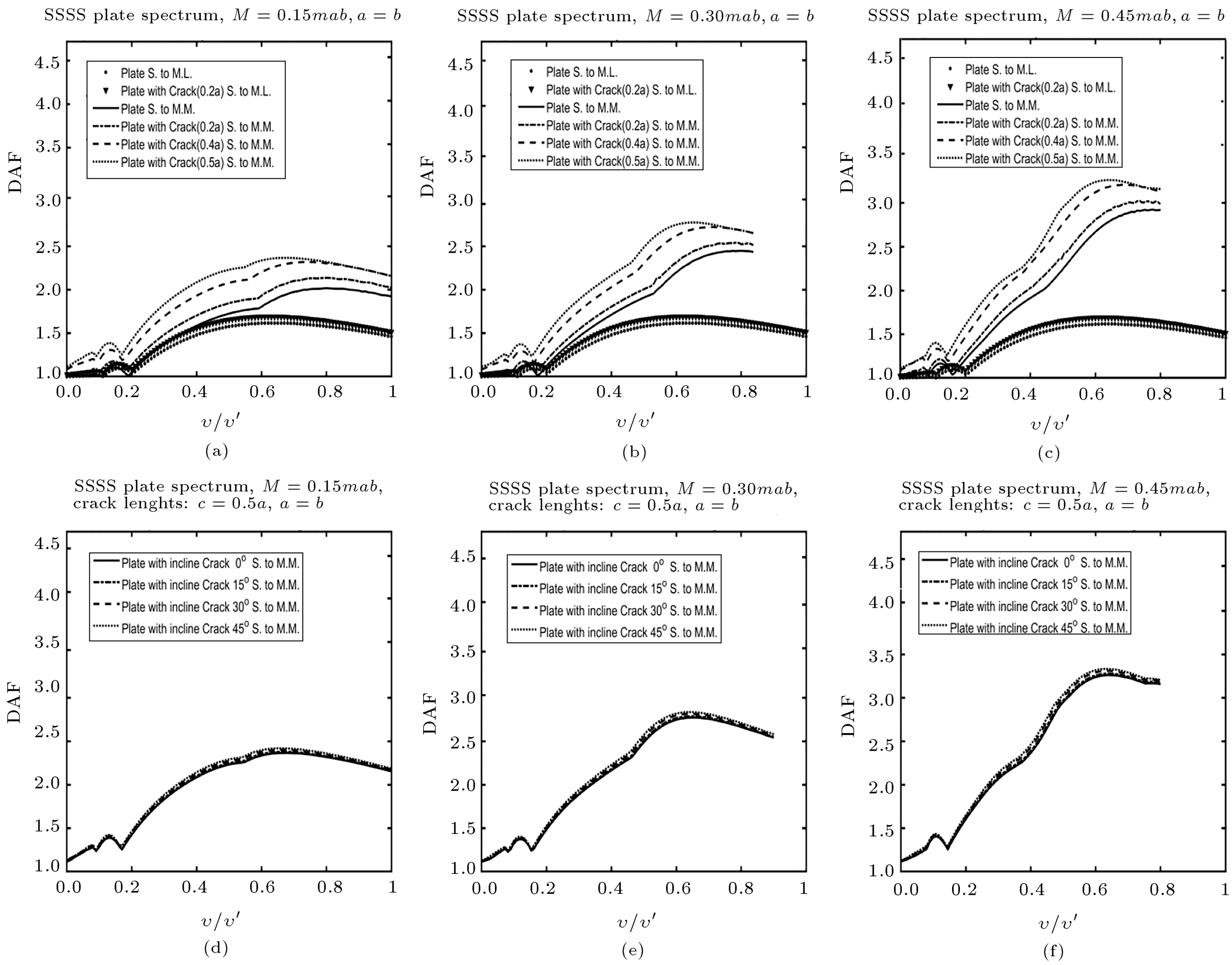

Figure 3. The effect of the inertia on DAFs of SSSS square plates with an internal crack due to alterations of velocities, mass weights, crack lengths, and inclined crack angles.

The process of obtaining the mass, and velocity limits of a moving mass on plates with various boundary conditions are resemble to the process of achieving the mass, and velocity limits of a moving mass on simple supported plates [43].

Figures 3–8 illustrate the maximum DAF curves of intact plates and cracked plates subjected to a moving load as well as a moving mass. Accordingly, the moving load spectra may remain similar at different mass weights. Of note, according to the problem formulation, because of the inertial effects, an induced damping matrix would emerge, while the mass and stiffness matrix components were changed, as well. Therefore, based on the moving load velocity and magnitude, the components of these matrices can be modified remarkably and, therefore, the dynamic behavior of the structure is affected. The moving mass spectra increase due to increase in the moving mass velocities as well as mass weights. Based on the figures, moving mass cases with diminutive weights and velocities can be approximate to the moving load cases as facilitated problems. Increase in the crack lengths and angle raises the inertial effects. As corner function formulas are expressed, crack lengths' variations and inclined crack angles' modifications, alter plates' mode shapes due to alterations of behaviors of stress singularities near the tips of the cracks. According to the figures, since the investigated cracks are constant cracks [44], increasing the crack lengths as well as the inclined crack angles is limited to the extent that stress intensity factors should be less than the critical stress intensity factor [44].

As shown in Figure 3, non-monotonous nonlinear relations exist between changing the DAFs of the plates and altering crack lengths and inclined crack angles. By increasing crack lengths and mass velocities at mass velocities less than $\approx 0.5v'$, the distances among the DAF curves increase slightly; for the mass velocities between $\approx 0.5v'$ and $\approx 0.6v'$, the DAF curves increase excessively and then, rise significantly; and for the mass velocities more than $\approx 0.6v'$, the distance among the DAF curves decreases obviously. By increasing the inclined crack angles, the DAF curves increase moderately. By increasing crack lengths and inclined

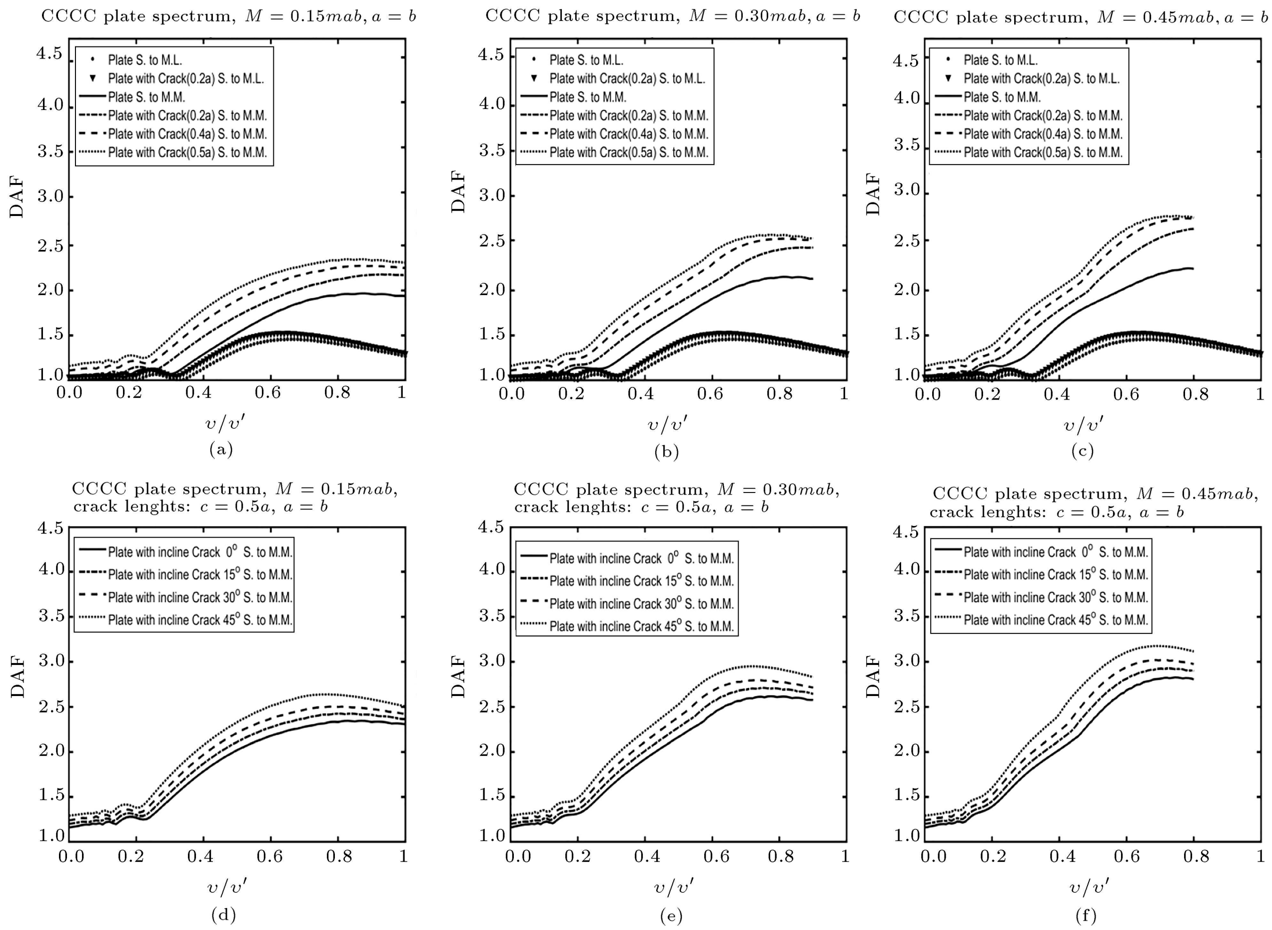

Figure 4. The effect of the inertia on DAFs of CCCC square plates with an internal crack due to alterations of velocities, mass weights, crack lengths, and inclined crack angles.

crack angles, the distances among the DAF curves increase because of inertial effects.

According to Figure 4, there are non-monotonous nonlinear relationships between altering the DAFs of the plates and modifying crack lengths and inclined crack angles. By increasing crack lengths, the distances among the DAF curves increase slightly. By increasing the inclined crack angles, the distances among the DAF curves increase moderately because of inertial effects. By increasing crack lengths and mass velocities, for the mass velocities less than $\approx 0.5v'$, the DAF curves increase gradually; for the mass velocities between $\approx 0.5v'$ and $\approx 0.6v'$, the DAF curves increase significantly; and for the mass velocities more than $\approx 0.6v'$, the DAF curves increase gently. According to the formulas of the proposed corner functions in Section 2, in the case of a cracked CCCC square plate, the order of the mentioned functions is more than that of similar functions in cracked SSSS square plate cases because of the geometrical boundary condition parameters in the formulas of corner functions. Therefore, by altering crack lengths and inclined crack angles, the differences among DAF curves in cracked CCCC square plate cases increase more than the mentioned curves in cracked SSSS square plate cases. However, according to the definition of the DAF, cracked CCCC square plate cases have lower DAF values than the cracked SSSS square plate cases.

Figure 5 illustrates non-monotonous nonlinear relations existing between altering the DAFs of the plates and modifying crack lengths and inclined crack angles. By increasing crack lengths, the distances among the DAF curves increase considerably and by increasing the inclined crack angles, the distances among the DAF curves increase noticeably because of the inertial effects. By increasing crack lengths and mass velocities, for the mass velocities less than $\approx 0.5v'$, the DAF curves increase slightly; for the mass velocities between $\approx 0.5v'$ and $\approx 0.6v'$, the DAF curves increase moderately; and for mass velocities more than $\approx 0.6v'$, the DAF curves increase substantially. In cracked SCSC square plate cases, an internal crack is parallel to the clamped edges or is assumed to be an inclined crack with an angle less than 45 degrees. Accordingly, these cracked SCSC square plates have smaller plates than the similar cracked CSCS square plates. The reason for this stiffness reduction could be observed obviously in the presented corner function formulas in Section 2.

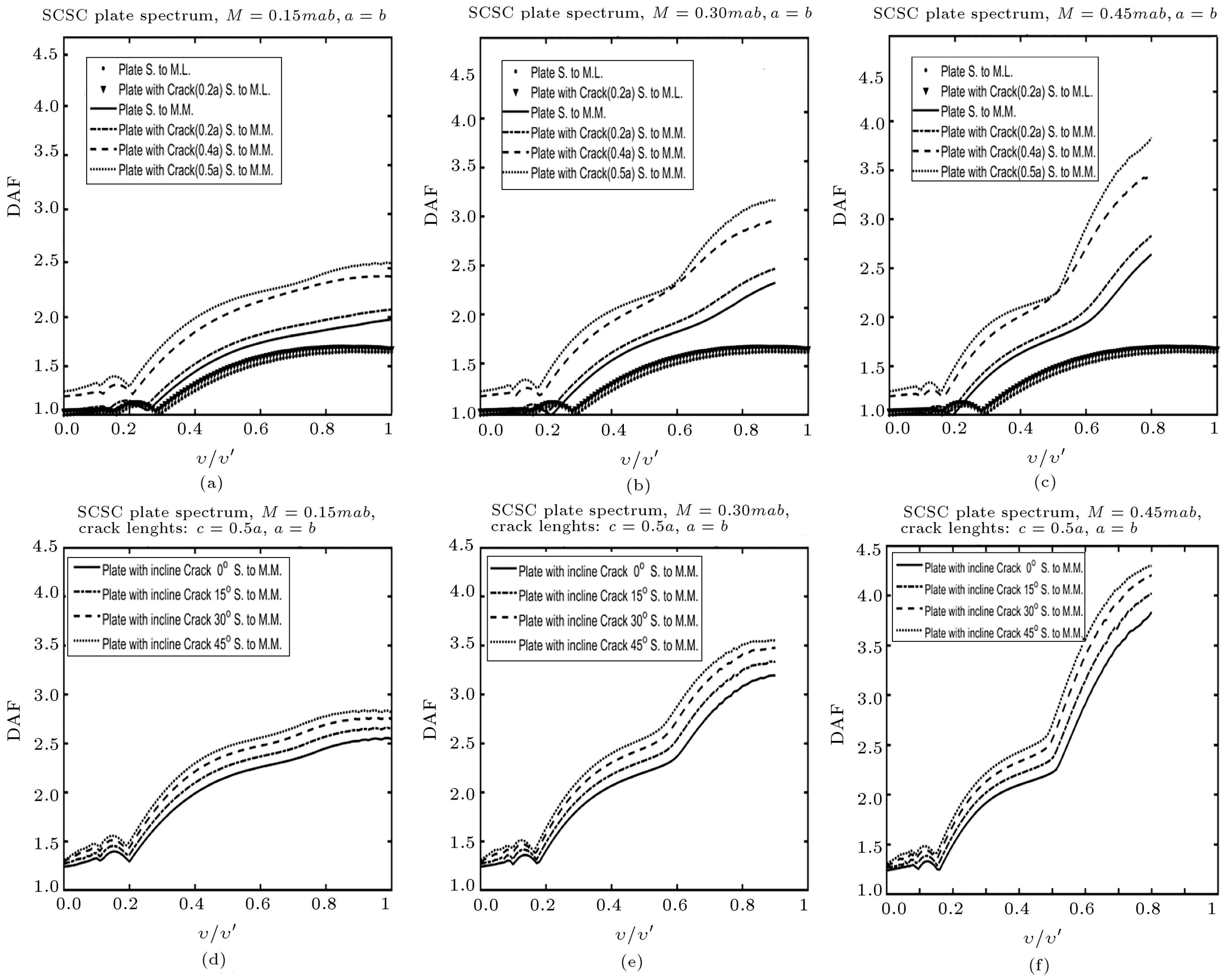

Figure 5. The effect of the inertia on DAFs of SCSC square plates with an internal crack due to alterations of velocities, mass weights, crack lengths, and inclined crack angles.

Furthermore, the order of the mentioned functions is more than the order of similar functions in the cracked SSSS square plate cases because of the geometrical boundary condition parameters in the corner function formulas. As mentioned earlier, given that DAF values are normalized ones, by changing crack lengths and inclined crack angles, DAF values in cracked SCSC square plate cases increase more than DAF values in the cracked SSSS square plate cases, and the difference among DAF curves in cracked SCSC square plate cases increases apparently.

As shown in Figure 6, the Winkler foundation leads to the reduction of the DAFs of the SCSC square plates with internal cracks resting on the Winkler foundation because of the reactions of the foundation, being proportional to deflections formulated as $p = KW(x, y, t)$ at any point of the plates. K is the modulus of the Winkler foundation. By increasing the moving mass weights, the DAFs of the plates increase slightly. There are non-monotonous nonlinear relationships between changing the DAFs of the plates and modifying crack lengths and inclined crack angles. By increasing crack lengths and inclined crack angles, the distances among the DAF curves increase slightly because of the inertial effects; for the mass velocities between $\approx 0.3v'$ and $\approx 0.5v'$, the DAF curves increase moderately and after the mass velocity at $\approx 0.5v'$, the DAF curves decrease slightly.

Figure 7 shows the non-monotonous nonlinear relations existing between changing the DAFs of the SCSC rectangular plates at an aspect ratio 1/2 and modifying crack lengths and inclined crack angles. By increasing crack lengths and inclined crack angles, the distances among the DAF curves increase obviously because of the inertial effects; and for mass velocities between $\approx 0.3v'$ and $\approx 0.7v'$, the DAF curves grow substantially; and after the mass velocity at $\approx 0.7v'$, the DAF curves increase gently. An internal crack in cracked plates is determined by its two tip coordinates employed in the corner function formulas as the ratio of a crack length to one side of cracked plate length c/a and the ratio of crack center locations to the cracked

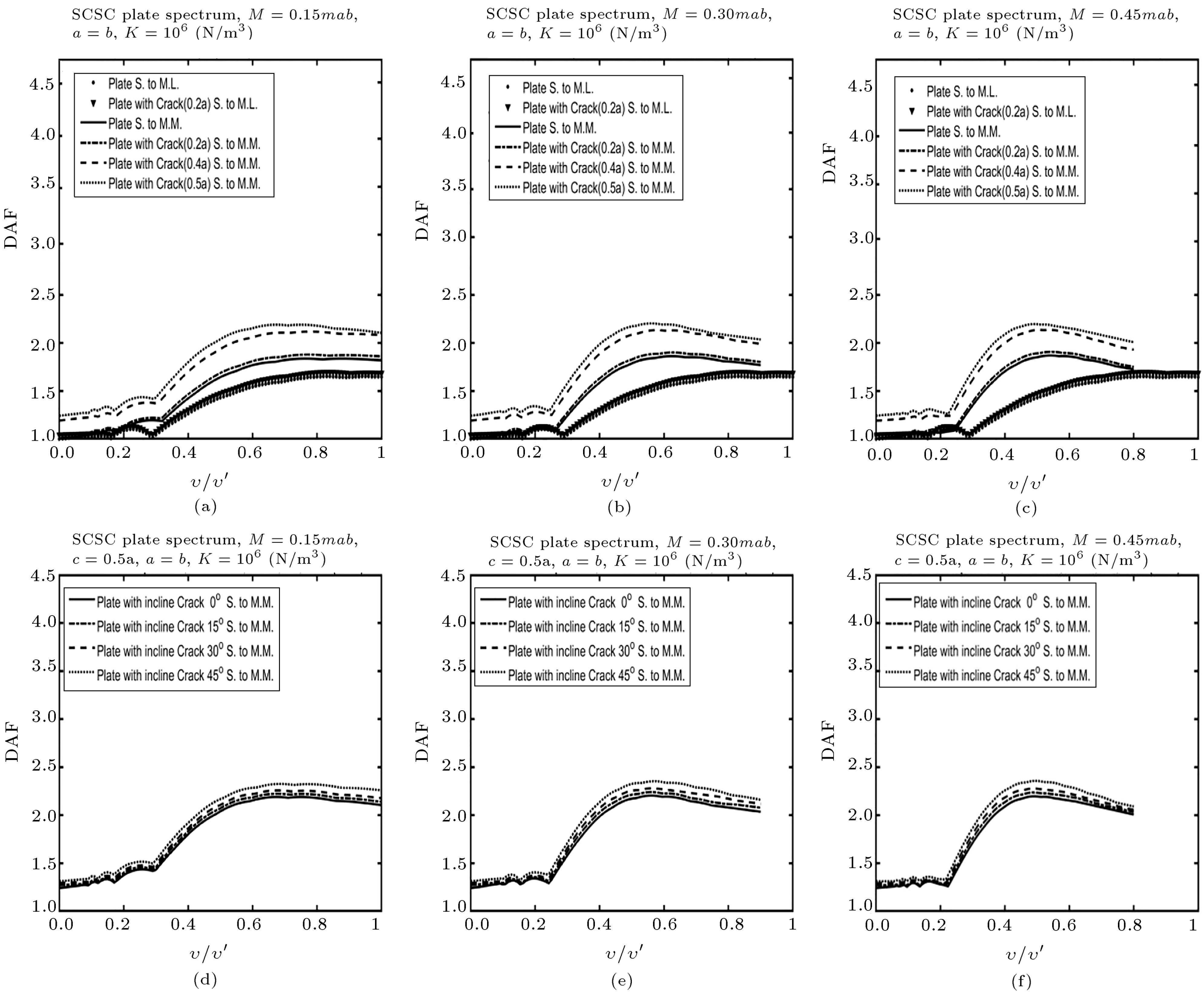

Figure 6. The effect of the inertia on DAFs of SCSC square plates with an internal crack resting on the Winkler foundation due to alterations of velocities, mass weights, crack lengths, and inclined crack angles.

plate edges a_0/a and b_0/b, as revealed in Sections 2 and 3. Therefore, an internal crack in cracked plates is defined by non-dimensional parameters. Accordingly, these cracked SCSC rectangular plates at an aspect ratio of 1/2 possess different non-dimensional parameters of crack orientations in comparison with the cracked SCSC square plate cases. Therefore, by changing similar crack lengths and inclined crack angles, DAF values and differences among DAF curves in the cracked SCSC rectangular plate at an aspect ratio 1/2 cases increase a little more than those in SCSC square plate cases.

As Figure 8 reveals, there are non-monotonous nonlinear relationships between modifying the DAFs of the rectangular plates with the aspect ratio 2 and increasing crack lengths and inclined crack angles. By increasing crack lengths as well as inclined crack angles, the distances among the DAF curves increase considerably because of the high inertial effects; for mass velocities between $\approx 0.3v'$ and $\approx 0.7v'$, the DAF curves increase significantly; and after the mass velocity $\approx 0.7v'$, the DAF curves decrease gradually. As mentioned earlier, the cracked plates with different shapes with similar crack lengths and inclined crack angles possess non-dimensional parameters of different crack orientations utilized in the corner function formulas. Therefore, by changing similar crack lengths and inclined crack angles, DAF values and differences among DAF curves in a cracked SCSC rectangular plate with the aspect ratio 2 increase considerably in comparison with those in the SCSC rectangular plate with the aspect ratio 1/2.

According to Figures 3–8, for the mass velocities larger than $\approx 0.2v'$, the inertial effects are not negligible, especially due to increase in moving mass weights, crack lengths, and inclined crack angles. There are non-monotonous nonlinear relations between altering DAF curves and modifying moving mass weights. According to the problem formulation, an initiated damping matrix emerge due to the inertial effects, while the mass and stiffness matrix components are changed, as

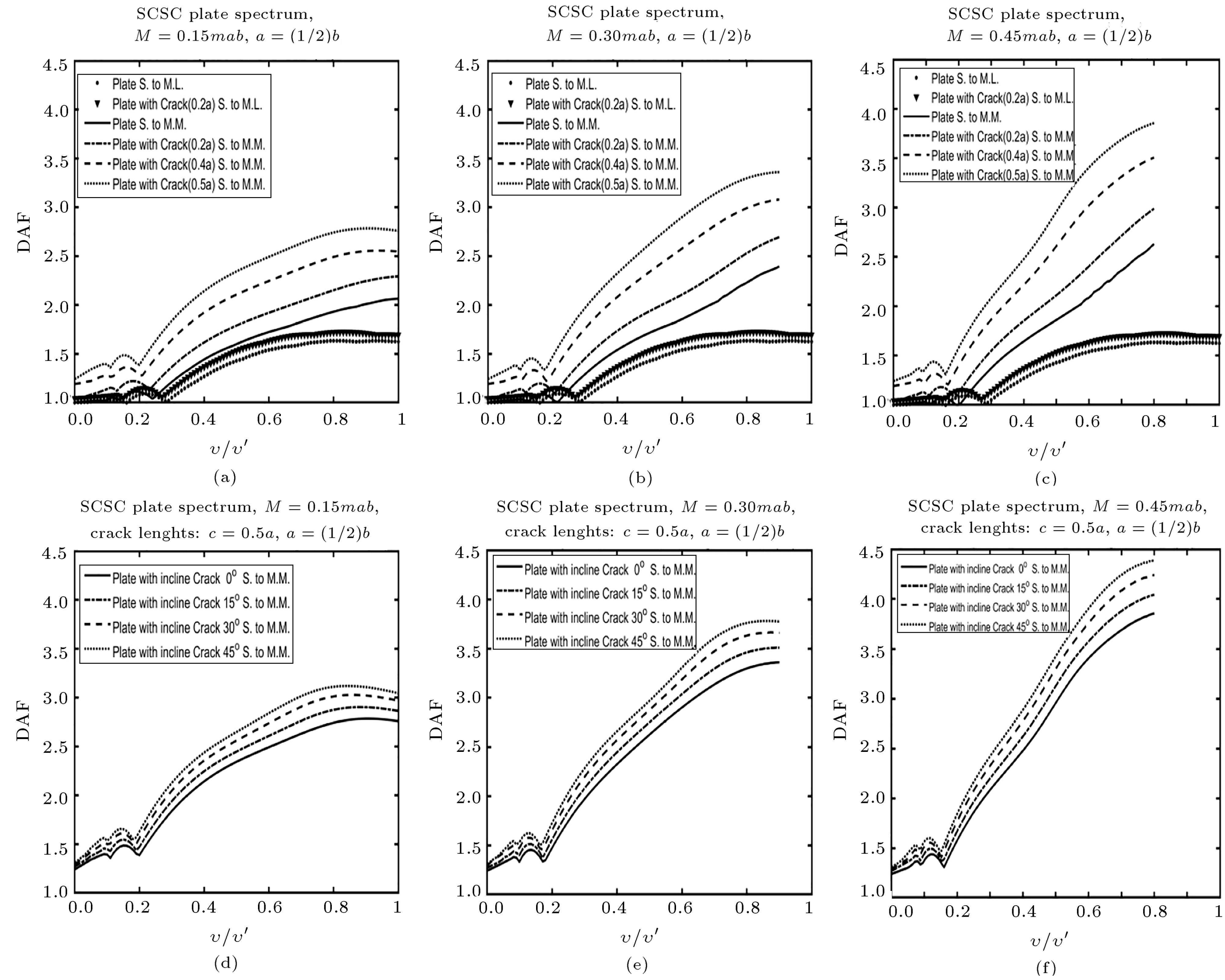

Figure 7. The effect of the inertia on DAFs of SCSC rectangular plates with the aspect ratio 1/2 and an internal crack due to alterations of velocities, mass weights, crack lengths, and inclined crack angles.

well. Therefore, based on the moving load velocity and magnitude, the components of these matrices are changed noticeably and therefore, the dynamic behavior of the structure is affected.

Figure 9 reveals the effects of crack lengths for different moving mass weights on the dynamic responses of cracked plates at constant velocities and various boundary conditions. As can be observed, there are non-monotonous nonlinear relationships between the maximum DAF values of the plates and the crack lengths for all cases. In the case of CCCC plates, the moving mass velocity $v = 0.7v'$ and the moving mass weights are equal to $0.3mab$ and $0.45mab$ for crack lengths more than $0.3a$ and the inclinations of the relevant curves are reduced, while for other cases, an increasing trend can be seen. Furthermore, in the case of SSSS plates and the moving mass velocity, $v = 0.7v'$, for the crack lengths more than $0.3a$, the inclinations of the relevant curves are reduced, while in other cases, the inclinations increase. For crack lengths less than $0.2a$ and more than $0.4a$, the inclinations of the relevant curves grow slightly, and between $0.2a$ and $0.4a$ the inclinations of the relevant curves increase noticeably. For other cases, for the crack lengths more than $0.3a$, the inclinations of the relevant curves are reduced. The elastically foundations, at any point of cracked plates, react proportional to the deflections. Therefore, for the case of elastically rested SCSC cracked plates, for moving mass velocity $v = 0.7v'$, the moving mass weight equals to $0.45mab$, and crack lengths more than $0.35a$, the inclinations of the relevant curves reduce slightly, and for other cases, the inclinations increase negligibly.

Figure 10 shows effects of inclined crack angles on the dynamic responses of plates for constant velocities, different moving mass weights, and various boundary conditions. There are non-monotonous nonlinear relations existing between the maximum DAF values of plates and inclined crack angles for all cases. In the case of the CCCC cracked plates, in a condition including inclined crack angles more than 25° and all moving mass weights, the inclinations of the relevant curves

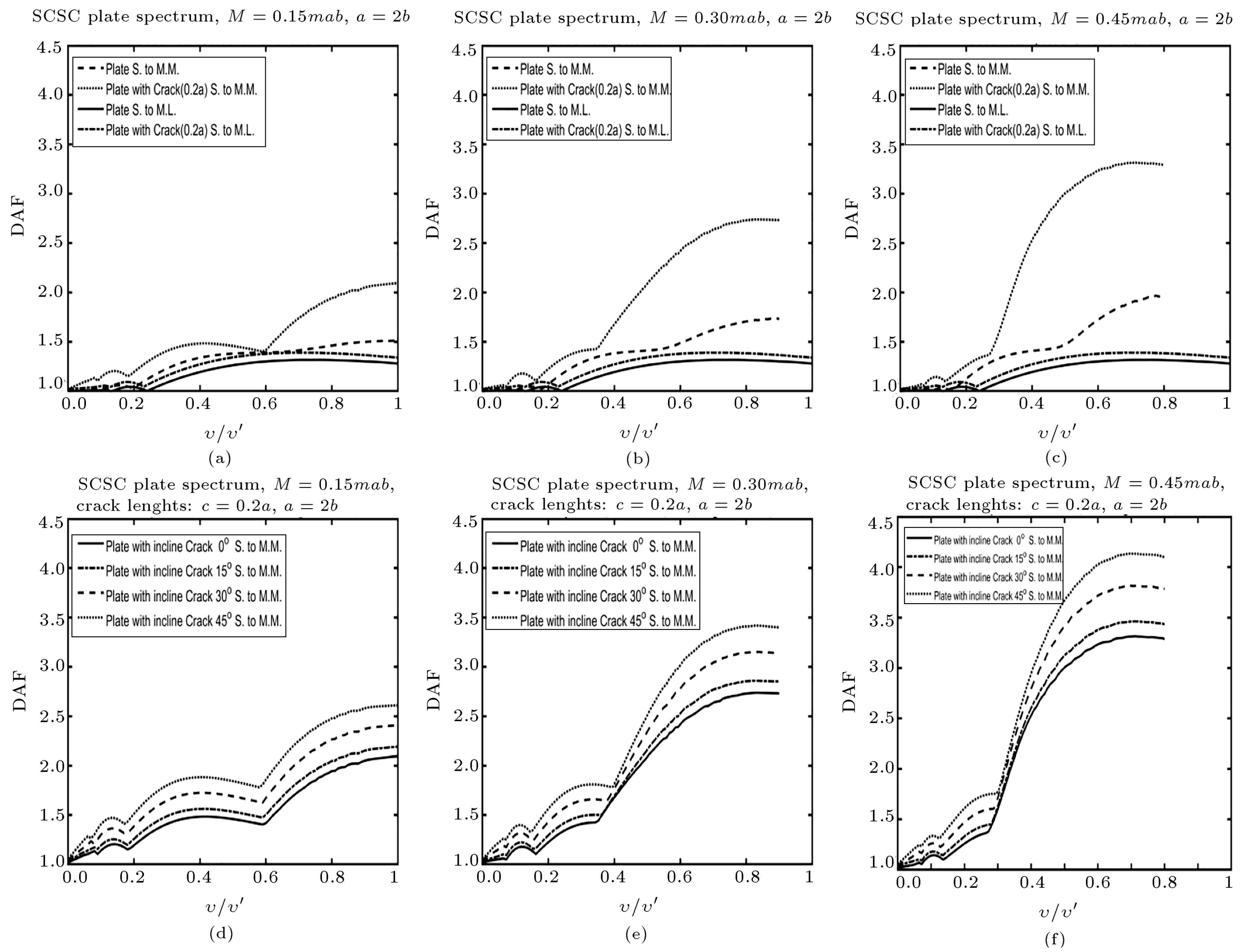

Figure 8. The effect of the inertia on DAFs of SCSC rectangular plates with the aspect ratio 2 and an internal crack due to alterations of velocities, mass weights, crack lengths, and inclined crack angles.

increase. Furthermore, in the case of SSSS cracked plates, for all moving mass weights, the inclinations of the relevant curves grow slightly. In the case of SCSC cracked plates, the moving mass velocity $v = 0.5v'$ and the moving mass weight are equal to $0.45mab$ and the inclination of the relevant curve increases considerably. In addition, for other cases, the inclinations of the relevant curves grow moderately. In the case of elastically rested SCSC cracked plates, the inclined crack angles more than $25°$ and all moving mass magnitudes led to elastically foundation reactions proportional to the deflections and the inclinations of the relevant curves increase inconsiderably.

Figure 11 illustrates the impact of plates' aspect ratios denoted by α for different moving mass weights on the dynamic responses of the plates at constant velocities. In the case of SCSC intact plates and cracked plates, similar to the case of SSSS intact plates investigated by Nikkhoo and Rofooei [30], there are constant relations between the aspect ratios and the maximum DAF values for plates for $\alpha \leq 1$. For $\alpha > 1$, there are non-monotonous nonlinear relationships existing between the maximum DAF values and aspect ratios for the plates in all cases because of direct effects of the ratio of plates' aspect to orthogonal polynomial formulations consisting of orthogonal polynomial formulas of intact plates, formula of corner functions, which are explained as plate displacements. Furthermore, inclinations of the relevant curves grow due to increase in the velocities and weights of the moving mass, especially in the case of cracked plates.

4. Conclusions

In this study, the differential equation of motion of an internally cracked rectangular plate subjected to a moving mass was considered. For the first time, the intact plate orthogonal polynomials, in combination with the well-known corner functions, were employed in the governing equation and the eigenfunction expansion method was utilized to solve the equation of motion of thin cracked plates with various boundary conditions as well as elastically rested thin cracked

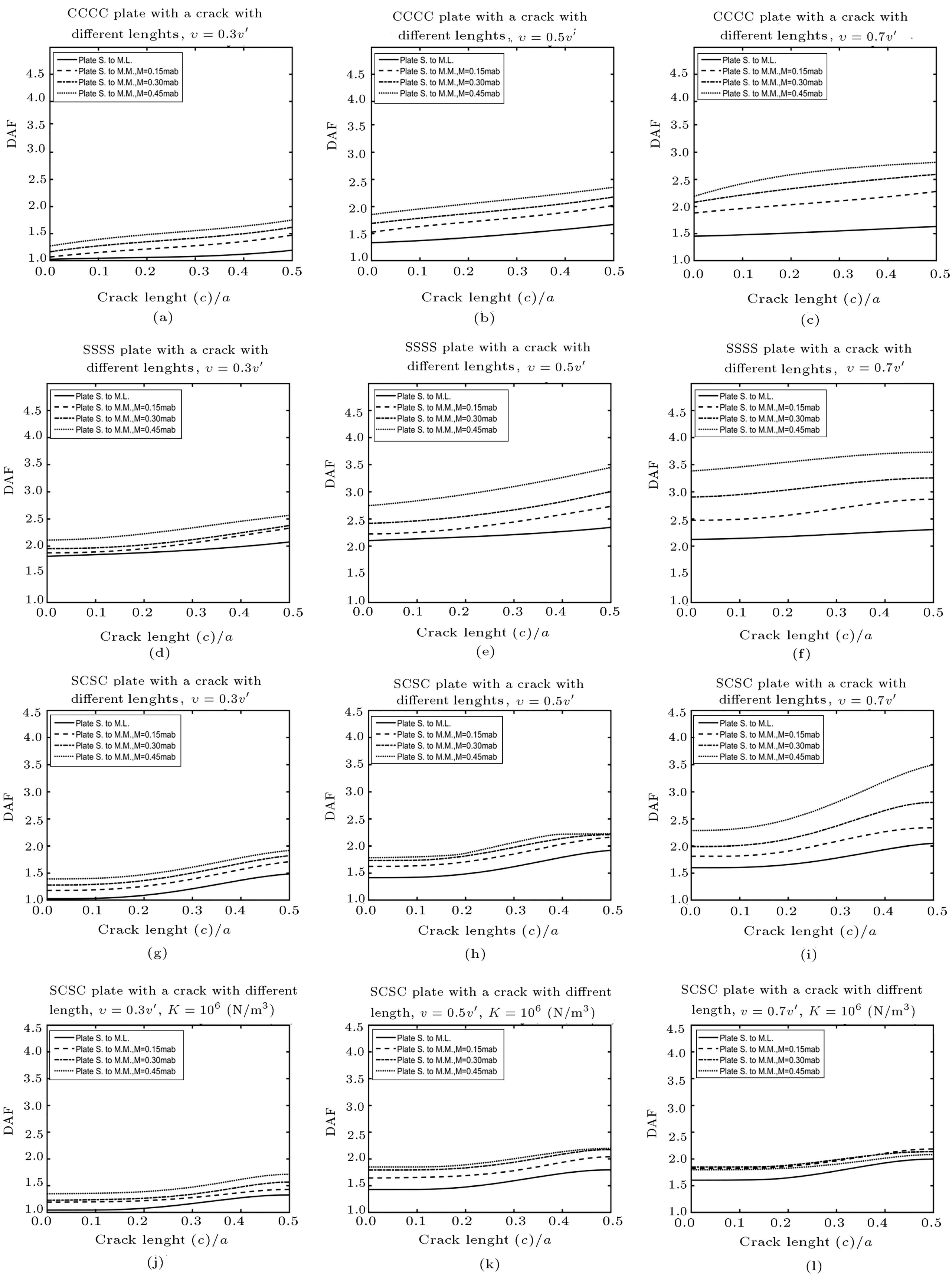

Figure 9. Effects of crack lengths on DAFs of cracked plates with CCCC, SSSS, and SCSC boundary conditions as well as elastically rested SCSC cracked plates.

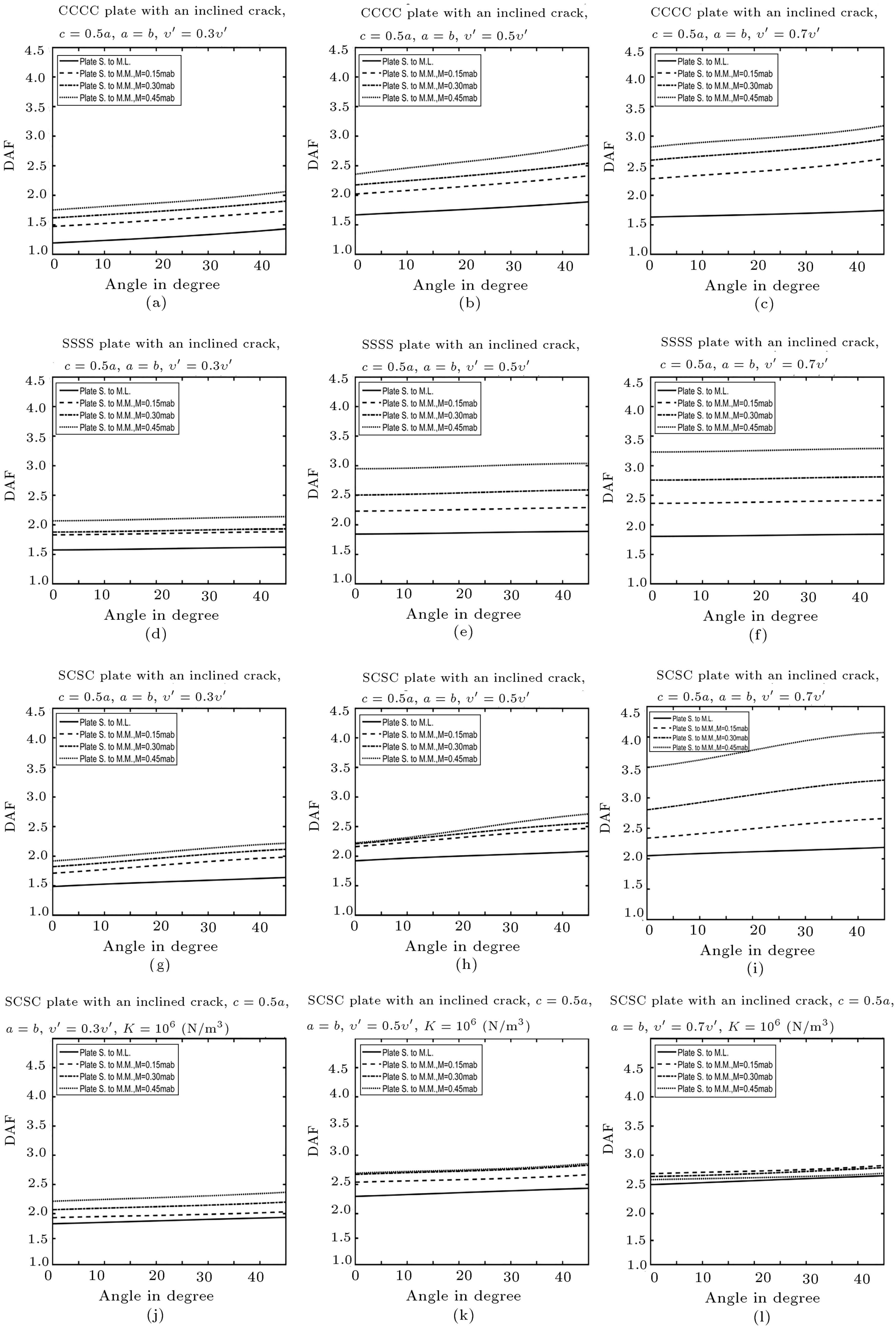

Figure 10. Effects of inclined crack angles on DAFs of cracked plates with CCCC, SSSS, and SCSC boundary conditions as well as elastically rested SCSC cracked plates.

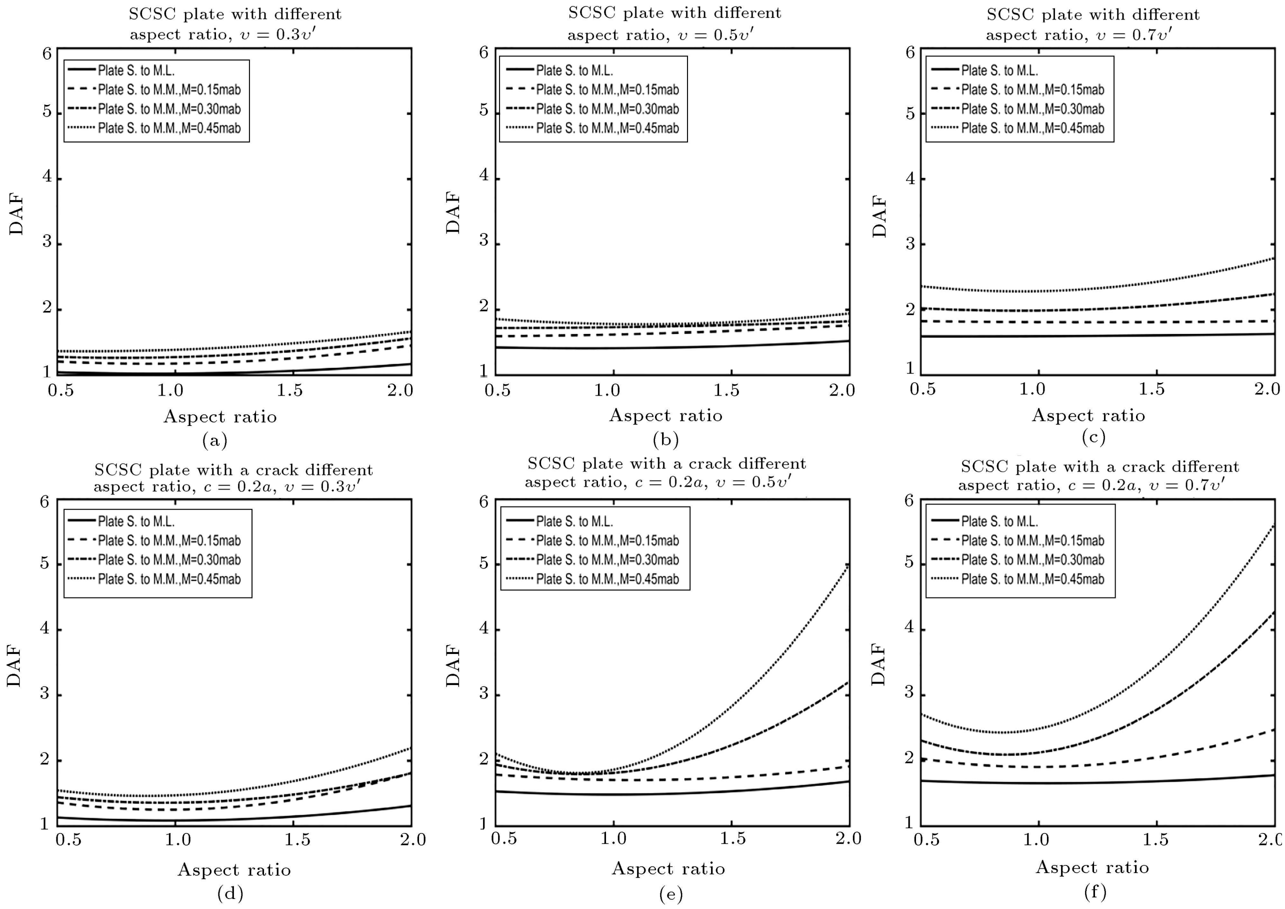

Figure 11. Effects of plates' aspect ratios on DAFs of intact plates as well as cracked plates with SCSC boundary conditions.

plates. The corner functions could determine the stress singularities near the tips of the crack and specify the discontinuities due to the crack line. The offered solutions created upper bounds for the accurate solution, which is a characteristic of an opportune numerical solution. Parametric studies were performed to investigate effects of moving mass weights, moving mass velocities, crack lengths, inclined crack angles, and the plates' aspect ratios on dynamic responses of cracked plates. Based on the results, by increasing the crack lengths and inclined crack angles, dynamic responses of SCSC cracked plates increased more than dynamic responses of CCCC, SSSS, and elastically rested SCSC cracked plates, while dynamic responses of elastically rested SCSC cracked plates increased less than dynamic responses of CCCC, SSSS, and SCSC cracked plates due to the inertial effects. Counter verse deflections proportional to reactions of the foundation, acting as a displacement controller, were deduced in elastically rested plate cases, in addition to moving mass deflections. According to the problem formulation, because of the inertial effects, an initiated damping matrix would emerge, while the mass and stiffness matrix components were changed, as well. Therefore, based on the moving load velocity and magnitude, the components of these matrices are altered significantly and therefore, the dynamic behavior of the structure is affected. In conclusion, there are non-monotonous nonlinear relationships between modifying the dynamic responses of cracked thin rectangular plates and elastically rested thin cracked plates with various boundary conditions and altering moving mass weights, moving mass velocities, crack lengths, inclined crack angles, and plates' aspect ratios.

References

1. Lynn, P.P. and Kumbasar, N. "Free vibration of thin rectangular plates having narrow cracks with simply supported edges", Developments in Mechanics. In. *Proceeding of the 10th Midwestern Mechanics Conference*, Colorado State University, Fort Collins, Colorado, **4**, pp. 911–928 (1967).

2. Stahl, B. and Keer, L.M. "Vibration and stability of cracked rectangular plates", *International Journal of Solids and Structures*, **8**, pp. 69–91 (1972).

3. Solecki, R. "Bending vibration of a simply supported rectangular plate with a crack parallel to one edge", *Engineering Fracture Mechanics*, **18**, pp. 1111–1118 (1983).

4. Qian, G.L., Gu, S.N., and Jiang, J.S. "A finite element model of cracked plates and application to vibration problems", *Computers and Structures*, **39**, pp. 483–487 (1991).

5. Krawczuk, M. "Natural vibrations of rectangular plates with a through crack", *Archive of Applied Mechanics*, **63**, pp. 491–504 (1993).

6. Bachene, M., Tiberkak, R., and Rechak, S. "Vibration analysis of cracked plates using the extended finite element method", *Archive of Applied Mechanics*, **79**, pp. 249–262 (2009).

7. Yuan, J. and Dickinson, S.M. "The flexural vibration of rectangular plate systems approached by using artificial springs in the Rayleigh–Ritz method", *Journal of Sound and Vibration*, **159**, pp. 39–55 (1992).

8. Liew, K.M., Hung, K.C., and Lim, M.K. "A solution method for analysis of cracked plates under vibration", *Engineering Fracture Mechanics*, **48**, pp. 393–404 (1994).

9. Lee, H.P. and Lim, S.P. "Vibration of cracked rectangular plates including transverse shear deformation and rotary inertia", *Computers and Structures*, **49**, pp. 717–718 (1993).

10. Huang, C.S. and Leissa A.W. "Vibration analysis of rectangular plates with side cracks via the Ritz method", *Journal of Sound and Vibration*, **323**, pp. 974–988 (2009).

11. Haung, C.S., Leissa, A.W., and Chan, C.W. "Vibrations of rectangular plates with internal cracks or slits", *International Journal of Mechanical Sciences*, **53**, pp. 436–445 (2011).

12. Haung, C.S., Leissa, A.W., and Li, R.S. "Accurate vibration analysis of thick, cracked rectangular plates", *Journal of Sound and Vibration*, **330**, pp. 2079–2093 (2011).

13. Riks, E., Bankin, C.C., and Brogen F.A. "The buckling of a central crack in a plate under tension", *Engineering Fracture Mechanics*, **43**, pp. 529–548 (1992).

14. Barut, A., Madenci, E., and Britt, V.O. "Starnes, J.R.: Buckling of a thin tension loaded composite plate with an inclined crack", *Engineering Fracture Mechanics*, **58**, pp. 233–248 (1997).

15. Brighenti, R. "Buckling sensitivity analysis of cracked thin plates under tension or compression", *Thin Walled Structures*, **43**, pp. 209–224 (2005).

16. Brighenti, R. "Buckling sensitivity analysis of cracked thin plates under membrane tension or compression loading", *Nuclear Engineering and Design*, **239**, pp. 965–980 (2009).

17. Zeng, H.C., Huang, C.S., Leissa, A.W., et al. "Vibration and stability of a loaded side- cracked rectangular plate via the MLS-Ritz method", *Thin-Walled Structures*, **106**, pp. 459–470 (2016).

18. Xue, J. and Wang, Y. "Free vibration analysis of a flat stiffened plate with side crack through the Ritz method", *Archive of Applied Mechanics*, **89**, pp. 2089–2102 (2019).

19. Xue, J., Wang, Y., and Chen, L. "Nonlinear vibration of cracked rectangular Mindlin plate with in- plane preload", *Journal of Sound and Vibration*, **481**, Art. 115437 (2020).

20. Huang, C.S., Lee, M.C., and Chang, M.J. "Vibration and buckling analysis of internally cracked square plates by the MLS-Ritz approach", *International Journal of Structural Stability and Dynamics*, **18**(9), Art. 1850105 (2018).

21. Xue, J., Wang, Y., and Chen, L. "Buckling and free vibration of a side- cracked Mindlin plate under axial in–plane load", *Archive of Applied Mechanics*, **90**, pp. 1811–1827 (2020).

22. Huang, C.S., Lee, H.T., Li, P.Y., et al. "Three-dimensional buckling analyses of cracked functionally graded material plates via the MLS-Ritz method", *Thin-Walled Structures*, **134**, pp. 189–202 (2019).

23. Huang, C.S., Lee, H.T., Li P.Y., et al. "Three- dimensional free vibration analyses of preloaded cracked plates of functionally graded materials via the MLS-Ritz method", *Materials*, **14**(24), Art. 7712 (2021).

24. Kiani, K. and Żur, K.K. "Vibrations of double-nanorod- systems with defects using nonlocal-integral-surface energy-based formulations", *Composit Structures*, **256**, pp. 113028–113043 (2021).

25. Mote, C.D. "Stability of circular plates subjected to moving load", *Journal of the Franklin Institute*, **290**, pp. 329–344 (1970).

26. Fryba, L., *Vibration of Solids and Structures Under Moving Loads*, Thomas Telford, London (1999).

27. Cifuentes, A. and Lalapet, S. "A general method to determine the dynamic response of a plate to a moving mass", *Computers and Structures*, **42**, pp. 31–36 (1992).

28. Shadnam, M.R., Mofid, M., and Akin, J.E. "On the dynamic response of rectangular plate with moving mass", *Thin Wall Structures*, **39**, pp. 797–806 (2001).

29. Rofooei, F.R. and Nikkhoo, A. "Application of active piezoelectric patches in controlling the dynamic response of a thin rectangular plate under a moving mass", *International Journal of Solids and Structures*, **46**, pp. 2429–2443 (2009).

30. Nikkhoo, A. and Rofooei, F.R. "Parametric study of the dynamic response of thin rectangular plates traversed by moving mass", *Acta Mechanica*, **223**, pp. 15–27 (2012).

31. Kiani, K. "Nonlocal continuum-based modeling of a nanoplate subjected to a moving nanoparticle. Part I: Theoretical formulations", *Physica E.*, **44**, pp. 229–248 (2011).

32. Kiani, K. "Nonlocal continuum-based modeling of a nanoplate subjected to a moving nanoparticle. Part II: Parametric studies", *Physica E.*, **44**, pp. 249–269 (2011).

33. Kiani, K. "Vibrations of biaxially tensioned- embedded nanoplates for nanoparticle delivery", *Indian Journal of Science and Technology*, **6**, pp. 4894–4902 (2013).

34. Nikkhoo, A., Hassanabadi, M.E., Azam, S.E., et al. "Vibration of a thin rectangular plate subjected to series of moving inertial loads", *Mechanics Research Communications*, **55**, pp. 105–113 (2014).

35. Rofooei, F.R, Enshaeian, A., and Nikkhoo, A. "Dynamic response of geometrically nonlinear, elastic rectangular plates under a moving mass loading by inclusion of all inertial components", *Journal of Sound and Vibration*, **394**, pp. 497–514 (2017).

36. Nikkhoo, A., Tafakor, R., and Mofid, M. "An exact solution to the problems of flexo-poro-elastic structures rested on elastic beds acted upon by moving loads", *Scientia Iranica*, **27**, pp. 2326–2341 (2019).

37. Chakraverty, S., *Vibration of Plates*, CRC Press, Boca Raton (2010).

38. Bhat, R.B. "Natural frequencies of rectangular plates using characteristic orthogonal polynomials in Rayleigh-Ritz method", *Journal of Sound and Vibration*, **102**(4), pp. 493–499 (1985).

39. Huang, C.S. and Huang, S.H. "Analytical solutions based on fourier cosine series for the free vibrations of functionally graded material rectangular mindlin plates", *Materials*, **13**(17), Art. 3820 (2020).

40. Timoshenko, S. and Winowsky-Krieger, S., *Theory of Plates and Shells*, McGraw–Hill, New York (1959).

41. Fryba, L. "History of winkler foundation", *Vehicle System Dynamics Supplement*, **24**, pp. 7–12 (1995).

42. Chopra, A.K., *Dynamics of Structures Theory and Applications to Earthquake Engineering in SI*, Pearson Prentice Hall, Upper Saddle River (2019).

43. Leissa, A.W., *Vibration of Plates*, US Government Printing Office, Washington, DC (1969).

44. Boresi, A.P. and Schmidt, R.J., *Advanced Mechanics of Materials*, John Wiley and Sons, Inc., New York (2002).

Biographies

Ali Nikkhoo was born in Tehran, Iran in 1978. He received a BSc degree in Civil Engineering from Isfahan University of Technology in 2000. Subsequently, he was awarded MSc and PhD degrees with a major in Structural Engineering as an honored student in 2002 and 2008, respectively. His current research focuses on dynamic behavior of beam and plate type structures under the action of moving forces as well as its active control and damage identification in such structural systems. To date, he has published more than 40 articles in peer-reviewed journals of mechanics and mathematics and has been the reviewer of more than 20 ISI journals.

Shirin Banihashemi is a PhD student in Construction Engineering at the Department of Civil Engineering University of Science and Culture (USC) in Tehran. She received a BSc degree in Civil Engineering from Khajeh Nasir al Din Toosi University of Technology (KNTU) in Tehran. After studing foundations of civil engineering, she involved herself in acoustics associated with constructions including building acoustics and noise controls, room acoustics, technical acoustics, psychoacoustics, electro acoustics, signal analyses, and theoretical acoustics. She also explored wave vibrations as well as dynamics of molecules, named as Brownian movement, at the Graz University of Technology in Austria. According to the relation between acoustical vibrations and structural vibrations, she continued her investigations at the USC in Tehran, obtaining an MSc degree in Structural Engineering. Her research interests are focused on acoustical vibrations as well as beam and plate form structures subjected to moving forces as well as moving random forces.

Keivan Kiani received a BSc degree in Civil Engineering from Isfahan University of Technology in 1999. Subsequently, he was awarded MSc and PhD degrees majoring in Structural Engineering from Sharif University of Technology in 2002 and 2010, respectively. The expert field of Dr. Kiani is modeling structures on nano and macro scales. His current research focuses on wave propagation as well as vibrations and dynamic instability of nanostructures using advanced elasticity theories. To date, he has published more than 110 ISI papers in a diverse range of journals of engineering, applied mathematics, and applied physics.